THE JOURNAL OF PHYSICAL CHEMISTRY A

Article

pubs.acs.org/JPCA

Dual Emission of a Novel (P,N) Re^{I} Complex: A Computational and Experimental Study on [*P,N*-{$(C_6H_5)_2(C_5H_4N)P$}$Re(CO)_3Br$]

Nancy Pizarro,[†] Mario Duque,[†] Eduardo Chamorro,[†] Santi Nonell,[‡] Jorge Manzur,[§,⊥] Julio R. de la Fuente,[∥] Germán Günther,[∥] Marjorie Cepeda-Plaza,[†] and Andrés Vega*[,†,⊥]

[†]Departamento de Ciencias Químicas, Facultad de Ciencias Exactas, Universidad Andres Bello, Quillota 980, Viña del Mar, Valparaíso, Chile

[‡]Institut Quimic de Sarrià, Universitat Ramon Llull, Via Augusta, 390, 08017 Barcelona, Spain

[§]Departamento de Ciencia de Los Materiales, Facultad de Ciencias Físicas y Matemáticas, Universidad de Chile, Av. Tupper 2069, Santiago, Chile

[∥]Facultad de Ciencias Químicas y Farmacéuticas, Departamento de Química Orgánica y Fisicoquímica, Universidad de Chile, Santos Dumont 964, Independencia, Chile

[⊥]Centro para el Desarrollo de la Nanociencia y la Nanotecnología, CEDENNA, Universidad de Santiago de Chile, Avda. Ecuador 3493, Estación Central, Santiago, Chile

Supporting Information

ABSTRACT: The spectroscopic, electrochemical, and photophysical properties of the new complex [*P,N*-{$(C_6H_5)_2(C_5H_4N)$-P}$Re(CO)_3Br$] are reported. The UV−vis spectrum in dichloromethane shows an absorption maximum centered at 315 nm and a shoulder at 350 nm. These absorption bands have been characterized to have MLCT character. Excitation at both wavelengths (maximum and shoulder) leads to an emission band centered at 550 nm. Cyclic voltammetry experiments show two ill-defined irreversible oxidation waves around +1.50 and 1.80 V that are assigned to Re^{I}/Re^{II} and Re^{II}/Re^{III} couples whereas an irreversible reduction signal centered at −1.80 V is likewise assigned to a ligand reduction process. These results support the proposal of the MLCT nature of the states implied by the emission of the complex. The luminescent decay fits to a biexponential function, where the lifetimes and emission quantum yields are dependent on the solvent polarity. DFT calculations suggest that $d\pi \rightarrow \pi^*_{pyridine}$ and $d\pi \rightarrow \pi^*_{phenyl}$ excited states may account for the existence of two decay lifetimes.

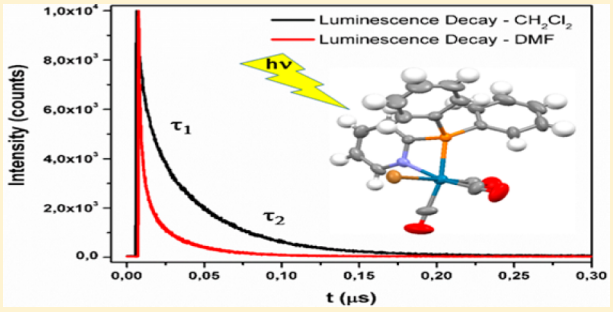

INTRODUCTION

Rhenium(I) tricarbonyl diimine complexes, [(N,N)Re-$(CO)_3$L], have been receiving considerable attention due to their interesting photophysical and photochemical properties, which can be modified by changing the nature of either the diimine ligand (N,N) or the L ligand (Cl, Br).[1−4] These structural changes have a direct effect on the excited state's character.[5] In a comparison to N,N-diimines, P,N-mixed complexes have been less studied so far, despite the fact that the presence of a heteroatom with different properties, i.e., hardness, coordinating ability, or trans-effect, adds new interesting features and possibilities which could be used to further tune the properties of complexes to a specific target application.[6−13] Even though the structures of bidentate P,N monometallic complexes of diphenylpyridylphosphine, $(C_6H_5)_2(C_5H_4N)P$, have been described for Ru,[14−19] Pt,[20,21] Tc,[22] Rh,[14,23] Ni,[24] W,[25−27] Re,[28−32] and Fe,[33] their photophysical properties remain largely unexplored. On the other hand, only a few mononuclear rhenium complexes bearing P,N-bidentate ligands have been described in the literature so far, namely, [{$(C_6H_5)_3P$}{*P,N*-$(C_6H_5)_2(C_5H_4N)P$}$ReCl_2$],[30] [{*O,N*-$(C_6H_5)_3P$}{$(C_6H_5)_2(C_5H_4N)PO$}$ReCl_3$],[29] and [{$(C_6H_5)_3P$}{P,N-$(C_6H_5)_2(C_5H_4N)P$}$Re(NO)_{0.87}Br_{2.13}$].[31] Among these compounds, only the absorption spectrum of [{$(C_6H_5)_3P$}{*P,N*-$(C_6H_5)_2(C_5H_4N)P$}$Re(NO)Cl_2$] has been reported. The absorption spectrum reveals a band in the visible region centered at 479 nm, which has been assigned to a $d \rightarrow \pi^*((C_6H_5)_2(C_5H_4N)P)$ metal to ligand charge transfer (MLCT) transition with the help of time-dependent density-functional theory (TD-DFT).[31] We have recently reported the synthesis and preliminary emission properties of a novel Re^{I} complex, [P,N-{$(C_6H_5)_2(C_5H_4N)P$}$Re(CO)_3Br$] (Scheme 1).[34]

Unlike complexes with N,N bidentate ligands, which have relatively high luminescent quantum yields on the order of 0.01−0.30 and lifetimes on the order of 100 ns,[3,35] our P,N

Received: December 18, 2014
Revised: March 30, 2015
Published: April 8, 2015

DOI: 10.1021/jp512614w
J. Phys. Chem. A 2015, 119, 3929−3935

Scheme 1. Schematic Representation of [*P,N*-{$(C_6H_5)_2(C_5H_4N)P$}$Re(CO)_3Br$]

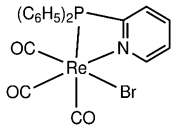

complex shows a surprisingly low emission quantum yield (lower than 0.001) and a biexponential emission decay with short luminescence lifetimes (on the order of nanoseconds).[34] Therefore, the aim of this work is to understand the underlying basis for such behavior, in order to be able to design new complexes for specific applications, for example, in the field of solar energy conversion. In the current work, we present the characterization of the spectroscopic, electrochemical, and photophysical properties of this complex, by comparing both experimental and computational results.

RESULTS AND DISCUSSION

i. Cyclic Voltammetry. Figure 1 illustrates the cyclic voltammogram of a 1.0 mM solution of [*P,N*-{$(C_6H_5)_2(C_5H_4N)P$}$Re(CO)_3Br$] in dichloromethane using 0.1 M tetra(*n*-butyl)ammonium perchlorate. Two irreversible oxidation processes with similar peak current and anodic peak potentials at ca. +1.50 and +1.80 V are observed during a positive potential scan initiated at 0.0 V. With the switch of the potential scan at +1.80 V, a reduction wave is observed at ca. 0.63 V with no coupled oxidation. If the potential is scanned initially in the negative direction, an irreversible reduction process is observed at −1.75 V. It is reasonable to propose that the oxidation processes correspond to the two consecutive metal-centered one-electron transfers Re^{I}/Re^{II} and Re^{II}/Re^{III}, as observed for [Re(1,2-bis(dimethylphosphino)ethane)$_3$].[36] An example of a complex displaying a P,N coordination environment is found for [(4,7-phenyl-1,10-phenanthroline)(P-$(C_6H_5)_3)_2Re(CO)_2$]{$B(C_6H_5)_4$}.[37] The irreversibility of the oxidation process may be explained with the assumption that ligand dissociation follows oxidation of the rhenium center. The signal at ca. +0.63 V could be assigned to the reduction of the resulting oxidation product giving the starting Re^{I} complex, since the second oxidation scan reproduces the first one. The reduction observed at −1.75 V is probably ligand based, as previously reported for other N,N-Re^{I} complexes in the range −1.2 to −1.8 V.[35]

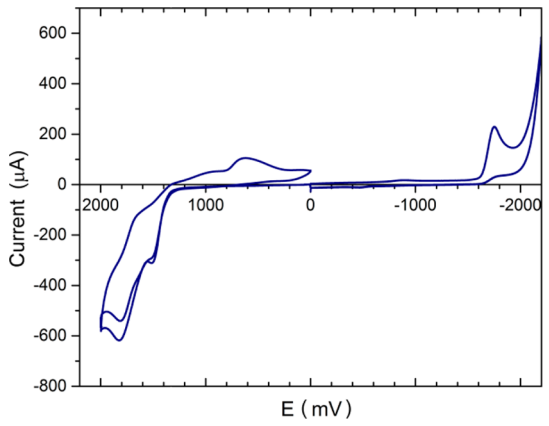

Figure 1. Cyclic voltammogram of [*P,N*-{$(C_6H_5)_2(C_5H_4N)P$}$Re(CO)_3Br$] measured in CH_2Cl_2 containing 0.10 mol L^{-1} $(C_4H_9)_4N^+ClO_4^-$ as supporting electrolyte with a glassy-carbon working electrode at a scan rate of 100 mV s^{-1}.

ii. Absorption Spectra and Computational Results. As shown in our previous work,[34] the [*P,N*-{$(C_6H_5)_2(C_5H_4N)P$}-$Re(CO)_3Br$] complex absorbs at 315 nm, with a shoulder around 355 nm in CH_2Cl_2 (Figure 2). In contrast, the

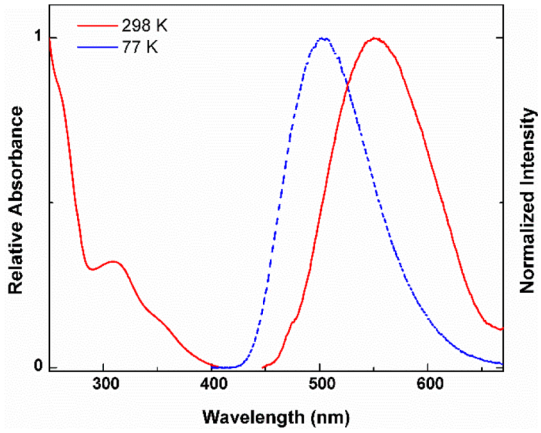

Figure 2. Absorption (left) and emission (right) spectra for [*P,N*-{$(C_6H_5)_2(C_5H_4N)P$}$Re(CO)_3Br$] at 298 K (solid line, CH_2Cl_2) and 77 K (dashed line). Excitation wavelength: 350 nm.

$(C_6H_5)_2(C_5H_4N)P$ ligand shows an intense absorption band centered at 257 nm, which has been assigned to a $\pi\pi^*$ transition due to the high molar absorptivity typically found for this kind of band.[38] The measured molar extinction coefficients are 5.0×10^3 and 2.5×10^3 L mol^{-1} cm^{-1} at 315 and 350 nm, respectively, which are comparable to those of related N,N complexes.[4] On the basis of these results, we assign both the 315 nm band and the 355 nm shoulder to a metal to ligand charge transfer (MLCT) transition from the Re^{I} d orbital with contribution of carbonyl π orbitals (Re^{I} d_π) to the ligand's π^* pyridyl orbital (π^*_{pyr}) being fully consistent with the results obtained from cyclic voltammetry.

Results from TD-DFT calculations support this explanation. Table 1 summarizes the main computed transitions with their respective energies, wavelengths, and oscillator strengths, together with the orbitals implied. Figure 3 shows that the computed transitions overlapped the absorption spectra of [*P,N*-{$(C_6H_5)_2(C_5H_4N)P$}$Re(CO)_3Br$]. According to these calculations, transitions 1 and 2, located around 350 nm, are predicted mainly as transitions between the d_π-type orbitals,

Table 1. Summary of Energy, Wavelength, and Oscillator Strength[a]

no.	*E*/eV	λ/nm	*f*	major contributions
1	3.48	356	0.0016	HOMO → LUMO (90%)
2	3.51	353	0.0237	H − 1 → LUMO (89%)
3	3.74	332	0.0083	HOMO → L + 1 (76%)
4	3.80	326	0.0258	H − 1 → L + 1 (78%)
5	3.96	313	0.0014	H − 1 → L + 2 (51%) H − 1 → L + 3 (23%)
18	4.70	264	0.0331	H − 8 → LUMO (11%) H − 7 → LUMO (60%)

[a]Computed for observed transitions in the absorption spectra of [*P,N*-{$(C_6H_5)_2(C_5H_4N)P$}$Re(CO)_3Br$], together with the orbital implied.

DOI: 10.1021/jp512614w
J. Phys. Chem. A 2015, 119, 3929−3935

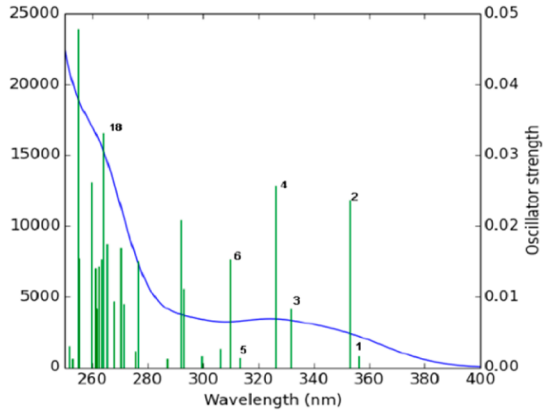

Figure 3. DFT computed transitions for $[P,N\text{-}\{(C_6H_5)_2(C_5H_4N)P\}Re(CO)_3Br]$ overlapped with the experimental absorption spectra.[34]

HOMO (H) and HOMO − 1 (H − 1), to a π^*-type orbital from the pyridinic ring of the P,N-ligand (LUMO), respectively. Additionally, transitions 3−5 (Table 1) account for the band at 315 nm involving a π^*-type orbital from either the pyridinic ring or the phenyl rings, being LUMO (L), LUMO + 1 (L + 1), and LUMO + 2 (L + 2), excited states very close in energy. Figure 4 depicts the TD-DFT computed

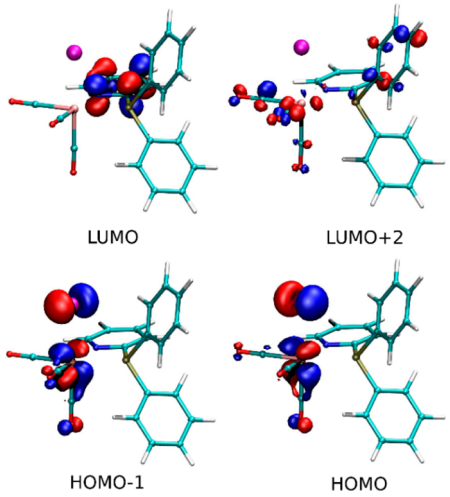

Figure 4. DFT computed frontier orbital HOMO − 1, HOMO, LUMO, and LUMO + 2 plots for $[P,N\text{-}\{(C_6H_5)_2(C_5H_4N)P\}Re(CO)_3Br]$. Complete scheme can be found in Supporting Information.

frontier orbitals plots for $[P,N\text{-}\{(C_6H_5)_2(C_5H_4N)P\}Re(CO)_3Br]$. We did not include L + 1 in the representation since this orbital is very close in energy and nature (π^*-type orbital from the pyridinic ring) to L. A complete scheme can be found in Supporting Information.

iii. Emission Properties. When excited at 315 or 350 nm, the title complex exhibits a broad emission band, with a maximum centered at 550 nm (2.26 eV) and a Stokes shift of 11 200 cm^{-1} (see Figure 2). Such a large shift is usually observed in MLCT transitions[38] and indicates a dramatic change in molecular dipole moment upon photoexcitation. The emission spectrum at 77 K remains structureless (Figure 2), which is also consistent with an MLCT emitting state, discarding emission centered on the ligand. The maximum of the emission band at low temperature is blue-shifted compared to that of the room-temperature spectrum, as can be seen in Figure 2, because the medium's rigidity prevents stabilization by solvent cage reorganization. Excitation and absorption spectra overlap closely, ensuring that the emission arises from the complex under study (see Supporting Information Figure S2). Other characteristics of MLCT transitions are emission maxima and quantum yields (Φ_{em}) dependent on the solvent polarity. Table 2 summarizes photophysical parameters of the complex.

Table 2. Emission Quantum Yields[a] and Lifetimes[a,b] of $[P,N\text{-}\{(C_6H_5)_2(C_5H_4N)P\}Re(CO)_3Br]$ at 298 K

solvent	Φ_{em}	τ_1/ns	τ_2/ns	Φ_Δ
CH_2Cl_2 (air)	5.0×10^{-4}	3.8 (87)	39.1 (13)	0.064
CH_2Cl_2 (Ar)	6.7×10^{-4}	4.0 (86)	45.6 (14)	
DMF (O_2)	$<10^{-4}$	2.9 (63)	14.2 (37)	
DMF (air)	2.5×10^{-4}	3.8 (66)	27.6 (33)	0.016
DMF (Ar)	5.7×10^{-4}	5.9 (60)	37.2 (40)	

[a]Errors were lower than 10%. [b]λ_{exc} = 400 nm and λ_{obs} = 560 nm. Values in parentheses are amplitudes in percent contribution from each decay component.

In aerated CH_2Cl_2 and DMF, emission quantum yields are 5.0×10^{-4} and 2.5×10^{-4}, respectively, 2 orders of magnitude smaller than the ones reported for related N,N complexes.[4] The DFT result confirms that the emission comes mainly from the frontier orbitals, and the fact that excited state geometry differs greatly from the ground state molecular geometry is consistent with such a large Stokes shift.

We have also examined the emission decay kinetics. It can be adequately modeled by a biexponential function having a fast component and a slow component, τ_1 and τ_2, respectively (Table 2). Both lifetimes are shortened with an increase in the polarity of the solvent. The luminescence decay profile is shown in Figure 5. The lifetime values are considerably shorter

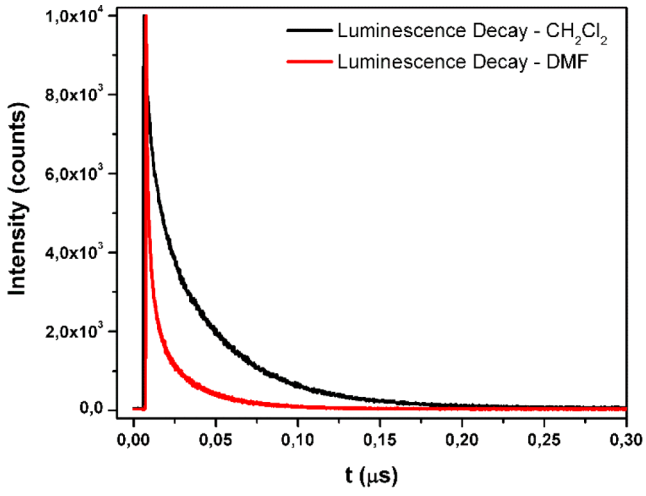

Figure 5. Luminescence decay curves of $[P,N\text{-}\{(C_6H_5)_2(C_5H_4N)P\}Re(CO)_3Br]$ followed at 560 nm after excitation at 400 nm in CH_2Cl_2 (black) and DMF (red).

compared to those found for some related N,N-complexes, usually in the range of several hundreds of nanoseconds,[35] which is in accordance with the low quantum yield observed. A decay described by a multiexponential fit is often associated with emission from more than one or many excited states.[39,40] For the case of $[P,N\text{-}\{(C_6H_5)_2(C_5H_4N)P\}Re(CO)_3Br]$, DFT calculations show that the $d\pi \rightarrow \pi^*_{pyr}$ excited state is very close

DOI: 10.1021/jp512614w
J. Phys. Chem. A 2015, 119, 3929−3935

in energy to the $d\pi \rightarrow \pi^*_{phenyl}$ state, which would explain the dual nature of the measured emission. The first component, τ_1, would correspond to the fast one, which is less sensitive to the polarity change than the slow component τ_2, whose value decreases around 70% in DMF compared to CH_2Cl_2. With this consideration, the fast component could be assigned to the emissive state involving the π^*_{phenyl} orbitals, while the slow one corresponds to $d\pi \rightarrow \pi^*_{pyr}$. This kind of dual emission has been observed for other rhenium complexes with phosphine ligands.[41] In order to analyze the energy associated with each emissive state, we obtained a time-resolved emission spectrum (TRES) for the complex, which is shown in Figure 6. As can be

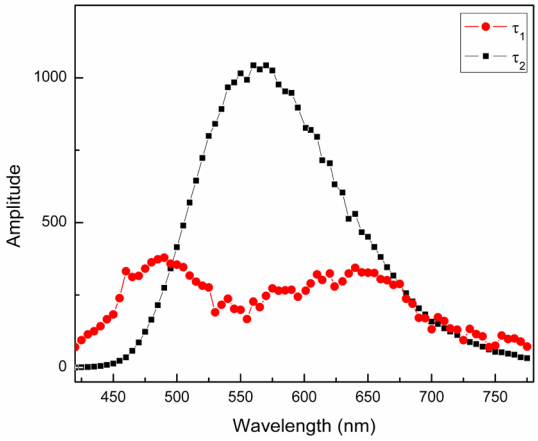

Figure 6. Time-resolved emission spectrum (TRES) of [*P,N*-{$(C_6H_5)_2(C_5H_4N)P$}$Re(CO)_3Br$] in CH_2Cl_2 after excitation at 400 nm. Slow (black) and fast (red) components.

observed in the plot, the fast component τ_1 seems to be associated with an emission maximum around 490 nm, while the slow component τ_2 shows an emission band centered at 565 nm. This result is consistent with both the existence of two emissive states and the assignment of the orbitals involved according to calculations shown in Table 1, where the π^*_{phenyl} orbitals are higher in energy than the π^*_{pyr} ones.

On the other hand, an increment of Φ_{em} and a lengthening of both lifetimes are observed in argon-saturated solutions, which can be attributed to quenching of both emissive excited states by oxygen (see Table 2). These results allow us to assign a triplet character to the MLCT states, which is compatible with the ultrafast intersystem crossing reported for Re^I tricarbonyl complexes.[33] Moreover, as shown in Figure 7a, laser flash photolysis at 355 nm reveals a broad transient absorption centered at 520 nm, which disappears with a biexponential profile, with lifetimes of 0.67 and >5.0 μs in argon-saturated solutions. The transient was not observed when the solutions were equilibrated with air, which probably implies that it corresponds to a state with triplet multiplicity (completely quenched in the presence of oxygen), or a species whose production is blocked by oxygen. This transient could arise from the emissive state $d\pi \rightarrow \pi^*_{pyr}$, because the slow component is strongly quenched by oxygen and could lead to photoproducts, i.e., a decarbonylated molecule. We did not examine the photochemistry of the complex, but there are many examples of carbon monoxide loss after a tricarbonyl complex's electronic excitation.[42−44] Therefore, the broad transient absorption at 520 nm might be assigned to a decarbonylated complex molecule.

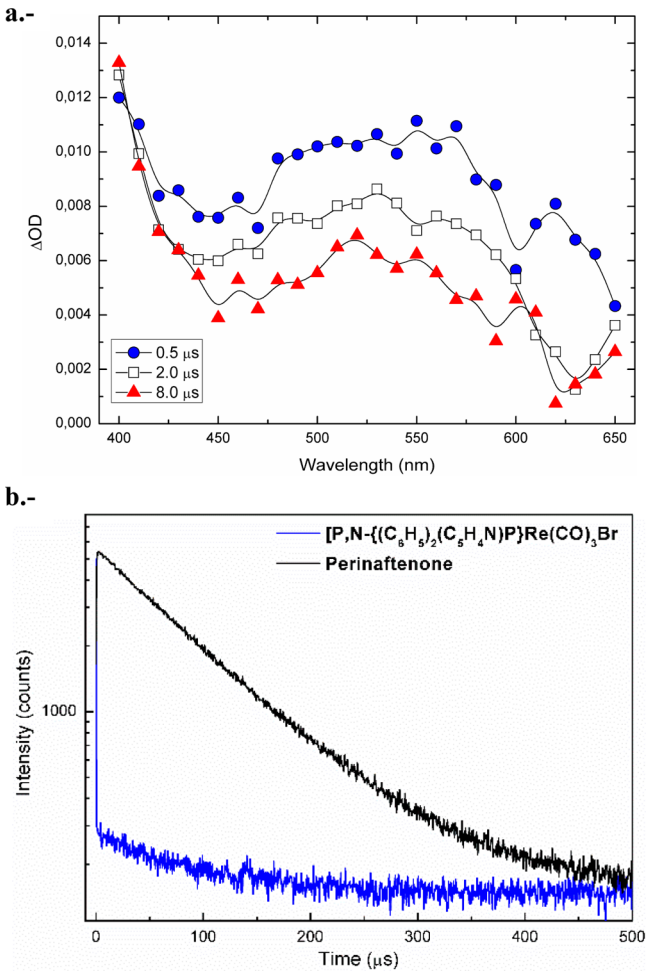

Figure 7. (a) Flash photolysis absorption spectrum of the complex [*P,N*-{$(C_6H_5)_2(C_5H_4N)P$}$Re(CO)_3Br$] in deareated CH_2Cl_2. (b) Singlet oxygen luminescence at 1270 nm after complex excitation at 355 nm in CH_2Cl_2 (blue). Reference was denoted in black.

As further evidence for the triplet character of the MLCT states, we found that, after irradiation at 355 nm, aerated solutions of the complex were able to generate singlet oxygen (Figure 7b). The production quantum yield (Φ_Δ) was found to be strongly dependent on the solvent polarity (see Table 2). This fact confirms the existence or presence of transients with triplet state multiplicity. According to the Wilkinson scheme and notations,[45] it is possible to propose that both initial transients, the shortest lived one (τ_1) and the longed lived one (τ_2), participate in the generation of singlet oxygen. With only kinetic considerations taken into account and the assumption of a singlet multiplicity, it is possible to calculate the proportion of each species quenched by ground state oxygen in oxygen-saturated solutions [considering that $P_{SQ}^{O_2}$ equals $k_{SQ}^{O_2}[O_2]/(k_{SD} + k_{SQ}^{O_2}[O_2])$]. With the highest value reported for singlet state quenching, 4×10^{10} M^{-1} s^{-1},[46,47] and the highest solubility of oxygen in organic solvents, 3 mM,[48] the proportion of quenched species is around 30% for the shortest lived transient and 80% for the longest one. According to lifetimes measured in DMF under oxygen-, air-, and argon-saturated conditions, reported in Table 2, and taking an oxygen solubility in DMF equal to 3.1 mM,[48] we can evaluate values for $k_{SQ}^{O_2}$ equal to 5.0×10^{10} and 1.4×10^{10} M^{-1} s^{-1} for each state.

DOI: 10.1021/jp512614w
J. Phys. Chem. A 2015, 119, 3929−3935

All this evidence suggests that the underlying mechanism of emission quenching for *P,N*-complexes is the nonradiative decay to the ground state. Nonradiative decay pathways would be facilitated by two main factors: (a) the proximity in energy between the MLCT excited state and the ground state with a gap of only 2.26 eV, in addition to the significant geometry distortion that is produced due to metal oxidation, both related to the energy gap law;[49] and (b) the conformational flexibility that the the pyridylphosphine ligand confers to the complex's efficient electronic-to-vibrational coupling modes, as compared to those of the rigid aromatic diimines in the N,N complexes.[50] In this context, both factors may be associated with an increase of the vibrational overlap between the ground and excited states, resulting from the combination of stretching modes present in this molecule, ν(Re−P), ν(Re−N), ν(Re−Br), and ν(C−O), with the concomitant faster radiationless decay.[2,51] With all the possible deactivation pathways upon excitation described above taken into account, a schematic energy diagram is proposed (Scheme 2).

Scheme 2. Schematic Energy Diagram Proposed for All the Possible Deactivation Pathways upon Excitation of [*P,N*-{$(C_6H_5)_2(C_5H_4N)P$}$Re(CO)_3Br$]

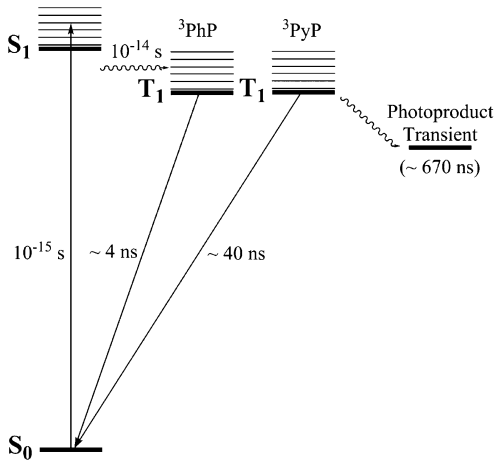

CONCLUSIONS

Light absorption by [*P,N*-{$(C_6H_5)_2(C_5H_4N)P$}$Re(CO)_3Br$] leads to an excited state having triplet MLCT character. The luminescent decay has been determined to be well-described by a biexponential fit with a short and a long component. The difference observed between both lifetimes, together with the sensitivity to solvent polarity, leads us to conclude that they come from different excited states. TD-DFT calculations validate the existence of two different states lying very close in energy, supporting the idea that the two emissions come from $d\pi \rightarrow \pi^*_{pyridine}$ and $d\pi \rightarrow \pi^*_{phenyl}$ excited states. In addition, these results allowed the identification of the nature of the participating orbitals. Therefore, the involvement of two emissive excited states of different nature would be responsible for the biexponential luminescent decay observed, which has not yet been reported for N,N complexes. Finally, we propose that the low emission quantum yield for this complex can be mainly attributed to conformational flexibility of the pyridylphosphine ligand, which confers to the complex efficient electronic-to-vibrational coupling modes, increasing the rate of radiationless decay.

EXPERIMENTAL WORK

i. Synthesis. The [*P,N*-{$(C_6H_5)_2(C_5H_4N)P$}$Re(CO)_3Br$] complex was prepared following a previously reported method.[34]

ii. Cyclic Voltammetry. Cyclic voltammograms at room temperature for [*P,N*-{$(C_6H_5)_2(C_5H_4N)P$}$Re(CO)_3Br$] were recorded in CH_2Cl_2 solutions (1.0 mM) using tetrabutylammonium perchlorate (0.10 M) as supporting electrolyte. Cyclic voltammograms were recorded at various sweep rates: 50, 100, 300, 500, and 600 mV s^{-1}. A vitreous carbon electrode was used as working electrode, a platinum electrode as auxiliary electrode, and a saturated calomel electrode as reference electrode. Iron ferrocene was used as internal standard.

iii. Spectroscopic and Photophysical Measurements. UV−vis spectra were recorded on an Agilent 8453 diode-array spectrophotometer in the range 250−700 nm in both aerated dichloromethane (CH_2Cl_2) and dimethylformamide (DMF) solutions. Emission spectra were measured in a Horiba Jobin-Yvon FluoroMax-4 spectrofluorometer either in both solvents mentioned previously at room temperature or in ethanol−methanol glass (4:1, v/v) at 77 K. Excitation spectra were recorded between 290 and 450 nm for an emission maximum of 550 nm. Luminescence lifetime measurements were carried out with the time correlated single photon counting technique using either an Edinburgh Instruments OB-900 or a PicoQuant Fluotime 200 fluorescence lifetime spectrometer. Nanosecond laser flash photolysis experiments were performed on argon-saturated dichloromethane solutions by excitation at 355 nm and sweeps of the absorption spectra between 400 and 600 nm. The instrument was described previously,[52−55] but now some additional accessories are available: a Continuum Surelite I 10 Hz Q-switched Nd:YAG laser is used while the signals are collected by a WaveSurfer 600 MHz LeCroy oscilloscope. Software written in National Instrument LabViews 8.0[56] controlled the laser, monochromator, and shutters, and captured the data that are fed to an Igor Pro 6.3[57] written program for treatment and display. Experiments were made in dichloromethane solutions which were either air-equilibrated or argon-saturated. Quantum yields were measured using procedures described in literature.[58]

iv. Computational Details. All geometry optimizations were performed at the B3LYP/6-31+G(d,p) level of theory using the Gaussian09 Rev C.01 package of programs (G09),[59] and started from geometry determined by means of X-ray diffraction.[34] The LANL2DZ basis set was used only for rhenium. Excited state calculations were performed within the time-dependent DFT methodology as implemented in G09. Solvent effects for simulating dichloromethane have been incorporated through the polarizable continuum model (PCM) using the integral equation formalism variant (IEFPCM).[60,61] Absorption and emission spectra were simulated from the above calculations using the GaussSum 3.0 suite of freely available processing tools. A full width at half-maximum (fwhm) of the Gaussian curves corresponding to 3000 cm^{-1} was employed to convolute both spectra. Representations for molecular orbitals were generated using the G09 cubegen tool and have been visualized using VMD and Povray 3.6 programs.[62,63]

DOI: 10.1021/jp512614w
J. Phys. Chem. A 2015, 119, 3929−3935

■ ASSOCIATED CONTENT

Supporting Information

Frontier orbital plots as well as excitation and absorption spectra for [*P,N*-{$(C_6H_5)_2(C_5H_4N)P$}$Re(CO)_3Br$]. This material is available free of charge via the Internet at http://pubs.acs.org.

■ AUTHOR INFORMATION

Corresponding Author

*E-mail: andresvega@unab.cl. Phone: +56322845192.

Author Contributions

The manuscript was written through contributions of all authors. All authors have given approval to the final version of the manuscript.

Notes

The authors declare no competing financial interest.

■ ACKNOWLEDGMENTS

The authors gratefully acknowledge partial financial support of Dirección de Investigación Universidad Andres Bello, Grant DI-111-12/R, and Comisión Nacional de Ciencia y Tecnología, Grants FONDECYT 1120865 and ACE-03. The authors are also thankful to Professor Russell Schmehl for his highly valuable suggestions. VMD was developed by the Theoretical and Computational Biophysics Group in the Beckman Institute for Advanced Science and Technology at the University of Illinois at Urbana−Champaign, http://www.ks.uiuc.edu/Research/vmd/.

■ REFERENCES

(1) Bullock, J. P.; Carter, E.; Johnson, R.; Kennedy, A. T.; Key, S. E.; Kraft, B. J.; Saxon, D.; Underwood, P. Reactivity of Electrochemically Generated Rhenium (II) Tricarbonyl A-Diimine Complexes: A Reinvestigation of the Oxidation of Luminescent Re(Co)3(A-Diimine)Cl and Related Compounds. *Inorg. Chem.* **2008**, *47*, 7880−7887.

(2) Smithback, J. L.; Helms, J. B.; Schutte, E.; Woessner, S. M.; Sullivan, B. P. Preparative Routes to Luminescent Mixed-Ligand Rhenium(I) Dicarbonyl Complexes. *Inorg. Chem.* **2006**, *45*, 2163−2174.

(3) Wenger, O. S.; Henling, L. M.; Day, M. W.; Winkler, J. R.; Gray, H. B. Photoswitchable Luminescence of Rhenium(I) Tricarbonyl Diimines. *Inorg. Chem.* **2004**, *43*, 2043−2048.

(4) Wrighton, M.; Morse, D. L. Nature of the Lowest Excited State in Tricarbonylchloro-1,10-Phenanthrolinerhenium(I) and Related Complexes. *J. Am. Chem. Soc.* **1974**, *96*, 998−1003.

(5) Cannizzo, A.; Blanco-Rodríguez, A. M.; El Nahhas, A.; Šebera, J.; Záliš, S.; Vlček, J. A.; Chergui, M. Femtosecond Fluorescence and Intersystem Crossing in Rhenium(I) Carbonyl−Bipyridine Complexes. *J. Am. Chem. Soc.* **2008**, *130*, 8967−8974.

(6) Kuang, S.-M.; Zhang, Z.-Z.; Wu, B.-M.; Mak, T. C. W. Synthesis of Fe-M Complexes (M = Mo, Mn, Fe, Co, Ni, Zn, Cd, Hg) Using Trans-Fe(Etphppy)2(Co)3 as an Organometallic Tridentate Ligand Molecular Structures of (Co)3fe(M-Etphppy)2mo(Co)3 and (Co)-3fe(M-Etphppy)2 cd(Scn)2 (Etphppy = 2-(Ethylphenylphosphino)-Pyridine. *J. Organomet. Chem.* **1997**, *540*, 55−60.

(7) Braunstein, P. Functional Ligands and Complexes for New Structures, Homogeneous Catalysts and Nanomaterials. *J. Organomet. Chem.* **2004**, *689*, 3953−3967.

(8) Braunstein, P.; Naud, F. Hemilability of Hybrid Ligands and the Coordination Chemistry of Oxazoline-Based Systems. *Angew. Chem., Int. Ed.* **2001**, *40*, 680−699.

(9) Espinet, P.; Soulantica, K. Phosphine-Pyridyl and Related Ligands in Synthesis and Catalysis. *Coord. Chem. Rev.* **1999**, *193−195*, 499−556.

(10) Guiry, P. J.; Saunders, C. P. The Development of Bidentate P,N Ligands for Asymmetric Catalysis. *Adv. Synth. Catal.* **2004**, *346*, 497−537.

(11) Helmchen, G.; Pfaltz, A. Phosphinooxazolinesa New Class of Versatile, Modular P,N-Ligands for Asymmetric Catalysis. *Acc. Chem. Res.* **2000**, *33*, 336−345.

(12) Newkome, G. R. Pyridylphosphines. *Chem. Rev.* **1993**, *93*, 2067−2089.

(13) Pfaltz, A.; Drury, W. J. Design of Chiral Ligands for Asymmetric Catalysis: From C2-Symmetric P,P- and N,N-Ligands to Sterically and Electronically Nonsymmetrical P,N-Ligands. *Proc. Natl. Acad. Sci. U.S.A.* **2004**, *101*, 5723−5726.

(14) Lalrempuia, R.; Carroll, P.; Rao Kollipara, M. Study of Reactivity Ofp-Cymene Ruthenium(Ii) Dimer Towards Diphenyl-2-Pyridylphosphine: Synthesis, Characterization and Molecular Structures of [(H6-P-Cymene)Rucl2(Pph2py)] and [(H6-P-Cymene)Rucl(Pph2py)]Bf4. *J. Chem. Sci.* **2004**, *116*, 21−27.

(15) Olmstead, M. M.; Maisonhat, A.; Farr, J. P.; Balch, A. L. Chelating 2-(Diphenylphosphino)Pyridine. Synthesis and Structure of Dichlorodicarbonyl[2-(Diphenylphosphino)Pyridine]Ruthenium(Ii). *Inorg. Chem.* **1981**, *20*, 4060−4064.

(16) Oshiki, T.; Yamashita, H.; Sawada, K.; Utsunomiya, M.; Takahashi, K.; Takai, K. Dramatic Rate Acceleration by a Diphenyl-2-Pyridylphosphine Ligand in the Hydration of Nitriles Catalyzed by Ru(Acac)2 Complexes. *Organometallics* **2005**, *24*, 6287−6290.

(17) Pfaltz, A.; Blankenstein, J.; Hilgraf, R.; Hörmann, E.; McIntyre, S.; Menges, F.; Schönleber, M.; Smidt, S. P.; Wüstenberg, B.; Zimmermann, N. Iridium-Catalyzed Enantioselective Hydrogenation of Olefins. *Adv. Synth. Catal.* **2003**, *345*, 33−43.

(18) Suzuki, T.; Kuchiyama, T.; Kishi, S.; Kaizaki, S.; Kato, M. Preparation, Crystal Structures, Electrochemical and Spectroscopic Properties of Bis(2(′)2 ′-Bipyridine)Ruthenium(Ii) Complexes Containing 8-(Diphenylphosphino)Quinoline or 2-(Diphenylphosphino)Pyridine. *Bull. Chem. Soc. Jpn.* **2002**, *75*, 2433−2439.

(19) Wajda-Hermanowicz, K.; Ciunik, Z.; Kochel, A. Syntheses and Molecular Structure of Some Rh and Ru Complexes with the Chelating Diphenyl (2-Pyridyl)Phosphine Ligand. *Inorg. Chem.* **2006**, *45*, 3369−3377.

(20) Farr, J. P.; Olmstead, M. M.; Wood, F.; Balch, A. L. Formation and Reactivity of Some Heterobinuclear Rhodium/Platinum Complexes with 2-(Diphenylphosphino)Pyridine as a Bridging Ligand. *J. Am. Chem. Soc.* **1983**, *105*, 792−798.

(21) Jain, V. K.; Jakkal, V. S.; Bohra, R. Methylplatinum(Ii) Complexes Containing 2-(Diphenylphosphino)Pyridine (Ph2ppy). Crystal and Molecular Structure of [Ptme(H2-Ph2ppy)(Ph2ppy)]-[Bph4]. *J. Organomet. Chem.* **1990**, *389*, 417−426.

(22) Freiberg, E.; Davis, W. M.; Nicholson, T.; Davison, A.; Jones, A. G. Reduction of the Pertechnetate Anion with Bidentate Phosphine Ligands. *Inorg. Chem.* **2002**, *41*, 5667−5674.

(23) Clarke, M. L.; Slawin, A. M. Z.; Wheatley, M. V.; Woollins, J. D. Synthesis and Structure of Novel Rhodium Complexes of Multi-Functionalised Amine-Phosphine Ligands. *J. Chem. Soc., Dalton Trans.* **2001**, 3421−3429.

(24) Polamo, M.; Laine, T. V. Crystal Structure of Dichlorobis 2-(Diphenylphospino)Pyridine Nickel(Ii), Nicl2 (C6h5)(2)(C5h4n)P (2). *Z. Kristallogr.* **2007**, *222*, 13−14.

(25) Baur, J.; Jacobsen, H.; Burger, P.; Artus, G.; Berke, H.; Dahlenburg, L. The Chemistry of New Nitrosyltungsten Complexes with Pyridyl-Functionalized Phosphane Ligands. *Eur. J. Inorg. Chem.* **2000**, *2000*, 1411−1422.

(26) Hirsivaara, L.; Haukka, M.; Pursiainen, J. Intramolecular Hydrogen-Bonding, Cation−Π, and Π-Stacking Interactions Affecting Cis/Trans Isomerization: Hexacarbonyltungsten Derivatives of Pyridyl-Substituted Arylphosphane Ligands. *Eur. J. Inorg. Chem.* **2001**, *2001*, 2255−2262.

(27) Nishide, K.; Ito, S.; Yoshifuji, M. Preparation of Carbonyltungsten(0) Complexes of 2-Pyridylphosphines Showing a Stepwise

DOI: 10.1021/jp512614w
J. Phys. Chem. A 2015, 119, 3929−3935

Coordination Pattern by Way of Monodentate to Chelate Mode. *J. Organomet. Chem.* **2003**, *682*, 79−84.
(28) Abram, U.; Alberto, R.; Dilworth, J. R.; Zheng, Y.; Ortner, K. Rhenium and Technetium Complexes with Diphenyl(2-Pyridyl)-Phosphine. *Polyhedron* **1999**, *18*, 2995−3003.
(29) Machura, B.; Jankowska, A.; Kruszynski, R.; Kłak, J.; Mroziński, J. Structural and Spectroscopic Studies on Rhenium(Iii) Diphenyl(2-Pyridyl)Phosphine Oxide Complexes. *Polyhedron* **2006**, *25*, 2663−2672.
(30) Machura, B.; Kruszynski, R. Synthesis, Crystal, Molecular and Electronic Structure of the [Re(No)Cl2(Pph3)(Pph2py-P,N)] Complex. *Polyhedron* **2006**, *25*, 1985−1993.
(31) Machura, B.; Kruszynski, R. Synthesis, Crystal, Molecular and Electronic Structure of the [Re(No) 0.87br 2.13(Pph 3)(Pph 2py-P,N)] Complex and Dft Calculations of [Re(No)Br 2(Pph 3)(Pph 2py- P,N)]. *J. Mol. Struct.* **2007**, *837*, 92−100.
(32) Saucedo Anaya, S. A.; Hagenbach, A.; Abram, U. Tricarbonylrhenium(I) and -Technetium(I) Complexes with Bis(2-Pyridyl)Phenylphosphine and Tris(2-Pyridyl)Phosphine. *Polyhedron* **2008**, *27*, 3587−3592.
(33) Nahhas, A. E.; Cannizzo, A.; Mourik, F. v.; Blanco-Rodríguez, A. M.; Záliš, S.; Vlček, J. A.; Chergui, M. Ultrafast Excited-State Dynamics of [Re(L)(Co)3(Bpy)]N Complexes: Involvement of the Solvent. *J. Phys. Chem. A* **2010**, *114*, 6361−6369.
(34) Venegas, F.; Pizarro, N.; Vega, A. Structural and Photophysical Properties of a Mononuclear Re(I) Complex:[P,N-{(C6h5)2(C5h5n)-P}Re(Co)3br]. *J. Chil. Chem. Soc.* **2011**, *56*, 823−826.
(35) Wallace, L.; Rillema, D. P. Photophysical Properties of Rhenium(I) Tricarbonyl Complexes Containing Alkyl- and Aryl-Substituted Phenanthrolines as Ligands. *Inorg. Chem.* **1993**, *32*, 3836−3843.
(36) Kirchhoff, J. R.; Allen, M. R.; Cheesman, B. V.; Ken-ichi, O.; Heineman, W. R.; Deutsch, E. Electrochemistry and Spectroelectrochemistry of [Re(1,2-Bis(Dimethylphosphino)Ethane)3]+. *Inorg. Chim. Acta* **1997**, *262*, 195−202.
(37) Kirillov, A. M.; Haukka, M.; Guedes da Silva, M. F. C.; Pombeiro, A. J. L. Synthesis, Characterization and Redox Behaviour of Mono- and Dicarbonyl Phosphane Rhenium(I) Complexes Bearing N-, N,N- and N,O-Type Ligands. *Eur. J. Inorg. Chem.* **2007**, *2007*, 1556−1565.
(38) Lakowicz, J. R. *Principles of Fluorescence Spectroscopy*; Springer: New York, 2006.
(39) Shaw, J. R.; Schmehl, R. H. Photophysical Properties of Rhenium(I) Diimine Complexes: Observation of Room-Temperature Intraligand Phosphorescence. *J. Am. Chem. Soc.* **1991**, *113*, 389−394.
(40) Magde, D.; Magde, M. D., Jr.; Glazer, E. C. So-Called "Dual Emission" for 3mlct Luminescence in Ruthenium Complex Ions: What Is Really Happening? *Coord. Chem. Rev.* **2015**, in press.
(41) Morimoto, T.; Ito, M.; Koike, K.; Kojima, T.; Ozeki, T.; Ishitani, O. Dual Emission from Rhenium(I) Complexes Induced by an Interligand Aromatic Interaction. *Chem.—Eur. J.* **2012**, *18*, 3292−3304.
(42) Koike, K.; Okoshi, N.; Hori, H.; Takeuchi, K.; Ishitani, O.; Tsubaki, H.; Clark, I. P.; George, M. W.; Johnson, F. P. A.; Turner, J. J. Mechanism of the Photochemical Ligand Substitution Reactions of Fac-[Re(Bpy)(Co)(3)(Pr3)](+) Complexes and the Properties of Their Triplet Ligand-Field Excited States. *J. Am. Chem. Soc.* **2002**, *124*, 11448−11455.
(43) Sato, S.; Sekine, A.; Ohashi, Y.; Ishitani, O.; Blanco-Rodriguez, A. M.; Vicek, A.; Unno, T.; Koike, K. Photochemical Ligand Substitution Reactions of Fac-[Re(Bpy)(Co)(3)Cl] and Derivatives. *Inorg. Chem.* **2007**, *46*, 3531−3540.
(44) Sato, S.; Matubara, Y.; Koike, K.; Falkenstrom, M.; Katayama, T.; Ishibashi, Y.; Miyasaka, H.; Taniguchi, S.; Chosrowjan, H.; Mataga, N.; et al. Photochemistry of Fac-[Re(Bpy)(Co)3cl]. *Chem.—Eur. J.* **2012**, *18*, 15722−15734.
(45) Wilkinson, F.; Helman, W. P.; Ross, A. B. Quantum Yields for the Photosensitized Formation of the Lowest Electronically Excited Singlet State of Molecular Oxygen in Solution. *J. Phys. Chem. Ref. Data* **1993**, *22*, 113−262.
(46) Wilkinson, F.; McGarvey, D. J.; Olea, A. F. Factors Governing the Efficiency of Singlet Oxygen Production During Oxygen Quenching of Singlet and Triplet States of Anthracene Derivatives in Cyclohexane Solution. *J. Am. Chem. Soc.* **1993**, *115*, 12144−12151.
(47) Abdel-Shafi, A. A.; Worrall, D. R. Mechanism of the Excited Singlet and Triplet States Quenching by Molecular Oxygen in Acetonitrile. *J. Photochem. Photobiol., A* **2005**, *172*, 170−179.
(48) James, H. J.; Broman, R. F. Modified Winkler Determination of Oxygen in Dimethylformamide: Oxygen Solubility as a Function of Partial Pressure. *Anal. Chim. Acta* **1969**, *48*, 411−417.
(49) Caspar, J. V.; Meyer, T. J. Application of the Energy Gap Law to Nonradiative, Excited-State Decay. *J. Phys. Chem.* **1983**, *87*, 952−957.
(50) Zipp, A. P.; Sacksteder, L.; Streich, J.; Cook, A.; Demas, J. N.; DeGraff, B. A. Luminescence of Rhenium(I) Complexes with Highly Sterically Hindered.Alpha.-Diimine Ligands. *Inorg. Chem.* **1993**, *32*, 5629−5632.
(51) Balk, R. W.; Stufkens, D. J.; Oskam, A. Characterization of Metal-to-Ligand Charge-Transfer and Intraligand Transitions of Fac-[Re(Co)3l(X)] Complexes [L = Di-Imine; X = Halide or Mn(Co)5] and Explanation of the Photochemistry of [Re(Co)3l{Mn(Co)5}] Using the Resonance Raman Effect. *J. Chem. Soc., Dalton Trans.* **1981**, 1124−1133.
(52) De la Fuente, J. R.; Aliaga, C.; Poblete, C.; Zapata, G.; Jullian, C.; Saitz, C.; Cañete, A.; Kciuk, G.; Sobarzo-Sanchez, E.; Bobrowski, K. Photoreduction of Oxoisoaporphines by Amines: Laser Flash and Steady-State Photolysis, Pulse Radiolysis, and Td-Dft Studies. *J. Phys. Chem. A* **2009**, *113*, 7737−7747.
(53) De la Fuente, J. R.; Cañete, Á.; Jullian, C.; Saitz, C.; Aliaga, C. Unexpected Imidazoquinoxalinone Annulation Products in the Photoinitiated Reaction of Substituted-3-Methyl-Quinoxalin-2-Ones with N-Phenylglycine. *Photochem. Photobiol.* **2013**, *89*, 1335−1345.
(54) De la Fuente, J. R.; Cañete, A.; Saitz, C.; Jullian, C. Photoreduction of 3-Phenylquinoxalin-2-Ones by Amines: Transient-Absorption and Semiempirical Quantum-Chemical Studies. *J. Phys. Chem. A* **2002**, *106*, 7113−7120.
(55) De la Fuente, J. R.; Neira, V.; Saitz, C.; Jullian, C.; Sobarzo-Sanchez, E. Photoreduction of Oxoisoaporphine Dyes by Amines: Transient-Absorption and Semiempirical Quantum-Chemical Studies. *J. Phys. Chem. A* **2005**, *109*, 5897−5904.
(56) *Labview, 8.0*; National Instruments Corporation, 2005.
(57) *Igor Pro, 6.3*; Wavemetrics: 2006.
(58) Crosby, G. A.; Demas, J. N. Measurement of Photoluminescence Quantum Yields. Review. *J. Phys. Chem.* **1971**, *75*, 991−1024.
(59) Frisch, M. J.; Trucks, G. W.; Schlegel, H. B.; Scuseria, G. E.; Robb, M. A.; Cheeseman, J. R.; Scalmani, G.; Barone, V.; Mennucci, B.; Petersson, G. A.; et al. *Gaussian 09*; Gaussian, Inc.: Wallingford, CT, 2009.
(60) Miertuš, S.; Scrocco, E.; Tomasi, J. Electrostatic Interaction of a Solute with a Continuum. A Direct Utilizaion of Ab Initio Molecular Potentials for the Prevision of Solvent Effects. *Chem. Phys.* **1981**, *55*, 117−129.
(61) Miertuš, S.; Tomasi, J. Approximate Evaluations of the Electrostatic Free Energy and Internal Energy Changes in Solution Processes. *Chem. Phys.* **1982**, *65*, 239−245.
(62) Humphrey, W.; Dalke, A.; Schulten, K. Vmd: Visual Molecular Dynamics. *J. Mol. Graphics* **1996**, *14*, 33−38.
(63) *Pov-Ray*, 3.7.0.

DOI: 10.1021/jp512614w
J. Phys. Chem. A 2015, 119, 3929−3935